PALEOCEANOGRAPHY

A 35-million-year record of seawater stable Sr isotopes reveals a fluctuating global carbon cycle

Adina Paytan[1]*, Elizabeth M. Griffith[2], Anton Eisenhauer[3], Mathis P. Hain[1], Klaus Wallmann[3], Andrew Ridgwell[4]

Changes in the concentration and isotopic composition of the major constituents in seawater reflect changes in their sources and sinks. Because many of the processes controlling these sources and sinks are tied to the cycling of carbon, such records can provide insights into what drives past changes in atmospheric carbon dioxide and climate. Here, we present a stable strontium (Sr) isotope record derived from pelagic marine barite. Our $\delta^{88/86}$Sr record exhibits a complex pattern, first declining between 35 and 15 million years ago (Ma), then increasing from 15 to 5 Ma, before declining again from ~5 Ma to the present. Numerical modeling reveals that the associated fluctuations in seawater Sr concentrations are about ±25% relative to present-day seawater. We interpret the $\delta^{88/86}$Sr data as reflecting changes in the mineralogy and burial location of biogenic carbonates.

S ecular variations in seawater radiogenic Sr isotope ratios (^{87}Sr/^{86}Sr) reflect changes in the relative input of Sr from weathering and hydrothermal activity and the ^{87}Sr/^{86}Sr composition of these fluxes (1), providing insights into links between silicate weathering and atmospheric partial pressure of CO_2 ($p$co$_2$) (2, 3). However, changes in seawater ^{87}Sr/^{86}Sr arise from multiple processes, complicating the relationship between ^{87}Sr/^{86}Sr and silicate weathering (4). By contrast, stable Sr isotopes ($\delta^{88/86}$Sr) respond to changes in both the ocean's Sr sources and carbonate sink (Fig. 1). The ocean Sr loss (output) is affected not only by net $CaCO_3$ deposition but also by varying relative proportions of $CaCO_3$ deposited in pelagic or neritic settings, with each environment being dominated by a different $CaCO_3$ mineralogy with differing Sr content. Specifically, changes in the deposition and/or dissolution of Sr-rich neritic $CaCO_3$ (i.e., aragonite) will result in a larger effect on the seawater Sr budget than changes in Sr-poor (calcitic) pelagic $CaCO_3$, such that $\delta^{88/86}$Sr is affected by changes in both the net rate of $CaCO_3$ burial and its neritic-pelagic partitioning (5, 6).

When combined, measurements of $\delta^{88/86}$Sr and ^{87}Sr/^{86}Sr thus offer the potential for detecting past changes in sources and sinks of Sr associated with continental weathering, hydrothermal activity, and carbonate deposition (Fig. 1) (5–7). Here, we reconstructed a 35-million-year (Myr) seawater $\delta^{88/86}$Sr (and ^{87}Sr/^{86}Sr) record from marine barite, and used a mass balance model (see the materials and methods section in the supplementary materials) to estimate

changes in seawater Sr concentration [Sr] resulting from imbalances between the total flux of Sr into and out of the ocean to infer past changes in carbonate deposition that could affect the C cycle.

Results

The measured ^{87}Sr/^{86}Sr values in 10 core-top barite samples reflect the present-day seawater

value [0.709165 ± 0.000005 (2σ)]. The average $\delta^{88/86}$Sr in these samples is −0.146‰ (relative to SRM987), reflecting an isotopic offset of −0.536‰ from modern seawater (8). The core-top samples encapsulate a total (max-min) range in $\delta^{88/86}$Sr of 0.038‰ (table S1), a range larger than the analytical uncertainty in our measurements (±0.02) (5). This variability is unlikely to be a temperature effect because the temperature at the depth of barite formation (~700 m) for these samples ranges from 1 to 14°C, and there is no correlation between $\delta^{88/86}$Sr and temperature (see discussion section in the supplementary materials). This offset is consistent with expectations based on previous work on synthetic and continental barite (9, 10) and data reported in Griffith et al. (11). This variability likely represents the range of $\delta^{88/86}$Sr in seawater during the time span represented by the upper 5 cm of sediments [up to 10,000 years (12)]. Therefore, rather than contemporary seawater $\delta^{88/86}$Sr, our core-top average reflects variability in the Holocene seawater composition of a few hundredths of a permille.

Down-core $\delta^{88/86}$Sr shows coherent changes spanning 0.1‰ (Fig. 2 and table S1). This is more than twice the range measured in core tops and more than five times the analytical
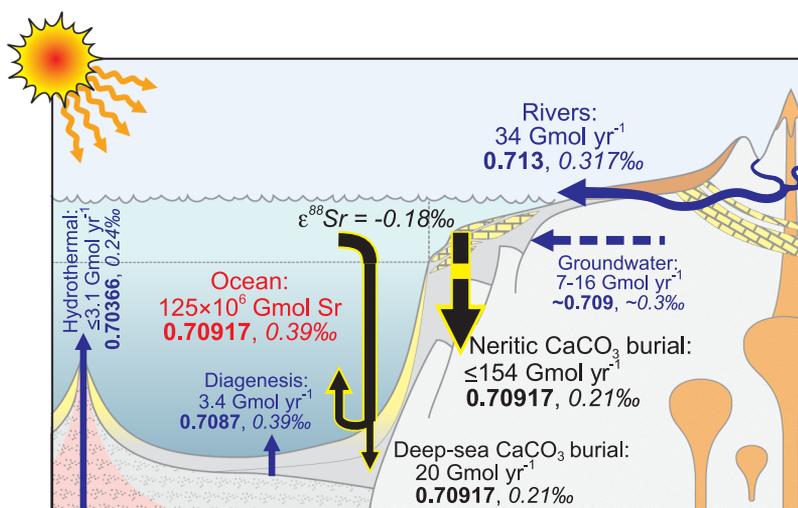

Fig. 1. Schematic diagram of the modern global Sr cycle illustrating the main controlling fluxes (Gmol Sr yr⁻¹) and ocean inventory. Mean isotope values are shown in bold for radiogenic Sr and in italics for stable Sr. The present-day average flux weighted river input to the ocean has an ^{87}Sr/^{86}Sr of 0.713 and $\delta^{88/86}$Sr of 0.317‰ (7), and this $\delta^{88/86}$Sr value corresponds to an average of different lithologies (silicate 0.58‰ and carbonates 0.18‰). Groundwater inputs have an average ^{87}Sr/^{86}Sr ratio of 0.709 and $\delta^{88/86}$Sr of ~0.3‰, and oceanic hydrothermal sources have an average ^{87}Sr/^{86}Sr ratio of 0.70366 and $\delta^{88/86}$Sr of 0.24‰ (7). The major oceanic Sr sink is the removal of Sr into marine $CaCO_3$, which preferentially incorporates the lighter Sr isotopes with an average isotope offset ε($\delta^{88/86}$Sr) of −0.18‰, resulting in average $CaCO_3$ $\delta^{88/86}$Sr of ~0.21‰ at present (6). Seawater ^{87}Sr/^{86}Sr at present is 0.70917 and the $\delta^{88/86}$Sr of seawater is 0.39‰, the latter being elevated above the $\delta^{88/86}$Sr of the inputs caused by preferential removal of light Sr isotopes into $CaCO_3$ (i.e., negative ε) driving seawater isotopically heavier. Dashed lines indicate more uncertain fluxes and isotopic compositions. Fluxes are compiled from the literature (see the supplementary materials). Note that available data suggest a large present-day Sr imbalance, so the Sr sink is substantially larger than the combined sources.

[1]Institute of Marine Science, University of California Santa Cruz, Santa Cruz, CA 95064, USA. [2]School of Earth Sciences, The Ohio State University, Columbus, OH 43210, USA. [3]GEOMAR Helmholtz Centre for Ocean Research Kiel, 24148 Kiel, Germany. [4]Department of Earth Sciences and Planetary Sciences, University of California Riverside, Riverside, CA 92521, USA.
*Corresponding author. Email: apaytan@ucsc.edu

uncertainty. Although the range is small, the consistency of the trend produced from samples from different locations offers strong evidence for a global seawater $\delta^{88/86}$Sr signal and is not an artifact of barite preservation (which would result in a unidirectional change with burial and different signatures at sites with different burial history). Furthermore, our down-core ^{87}Sr/^{86}Sr record, measured on the same samples, is consistent with the well-established seawater curve [Fig. 2A and table S1] (13). Even if we assume that core-top variability is noise (rather than being signal specific to the past few million years) and that this noise is present throughout the 35-Myr interval, it should be impossible to randomly generate the highly coherent record that we present (Fig. 2B). The temporal coherence in our record strongly argues against a random process.

Past seawater $\delta^{88/86}$Sr was reconstructed based on the barite record by applying a constant offset of 0.536‰. The resulting record ranges between ~0.3 and 0.4‰, which is within the range of Phanerozoic seawater $\delta^{88/86}$Sr derived from brachiopods (6). The highest values over the past 35 Myr occurred in the Early Oligocene; $\delta^{88/86}$Sr decreased by ~0.08‰ over the following ~20 million years, reaching a minimum in the Middle Miocene at ~15 Myr ago (Ma), after which time the $\delta^{88/86}$Sr increased by ~0.06‰ to a high in the Early Pliocene (~5 to 3.5 Ma), sharply decreasing by ~0.04‰ thereafter. These $\delta^{88/86}$Sr changes suggest that the marine Sr cycle since the Oligocene has been very dynamic, and that fluctuations were not unidirectional, as seen for the ^{87}Sr/^{86}Sr, which increased over this time interval.

Holocene and Pleistocene seawater Sr

Holocene core-top barites have a higher $\delta^{88/86}$Sr value (–0.146‰) than the average value of all down-core samples representing the past ~2.5 Myr (–0.186‰, corresponding to an average seawater value of 0.35‰), which themselves represent a range of –0.147 to –0.229‰ (table S1). In other words, seawater $\delta^{88/86}$Sr fluctuated considerably during the Holocene-Pleistocene (between ~0.31 and 0.39‰), with peak values around the core-top $\delta^{88/86}$Sr. Previous work based on the deviation of seawater ^{87}Sr/^{86}Sr from that expected from the total Sr input to the ocean measured in modern sources (terrestrial and hydrothermal) showed that seawater Sr sources and sinks are out of balance at present, which was attributed to intensified weathering related to Northern Hemisphere glaciation (5, 7, 14, 15) (fig. S1). The observed difference between our core-top $\delta^{88/86}$Sr and the long-term Pleistocene average directly documents this imbalance. Our record of the past 2.5 Ma, although documenting considerable fluctuations in $\delta^{88/86}$Sr, is only aliasing rather than

fully resolving the likely frequency of variability. Higher-resolution data from additional sites over this time interval are needed to better understand the nature of these fluctuations and their relationship to glacial-interglacial cycles. We suggest that these fluctuations are specific to the Pleistocene and stem from the rapid and large sea-level fluctuations resulting from Northern Hemisphere glaciations (see discussion section in the supplementary materials).

A 35-Myr record of seawater Sr

For most of the past 35 Myr, changes in seawater $\delta^{88/86}$Sr did not systematically correspond to changes in ^{87}Sr/^{86}Sr (Fig. 2), suggesting that the two records are largely controlled by different processes and implying that they can be modeled independently to the first order. Specifically, the most important processes that control oceanic $\delta^{88/86}$Sr (the uptake or release of Sr from neritic carbonates) impose only a secondary and small impact on ^{87}Sr/^{86}Sr by changing the bulk Sr inventory of the ocean. This is because the ^{87}Sr/^{86}Sr signature of neritic carbonates is nearly identical to that of seawater ^{87}Sr/^{86}Sr (Fig. 1).

To explain the variations in seawater $\delta^{88/86}$Sr, we derived the expression for seawater $\delta^{88/86}$Sr change over time, without making any steady-

state assumption, as follows (see derivation in the supplementary materials):

$$\frac{\Delta\delta_{SW}}{\Delta t} = \left(\frac{\delta_{IN} - \varepsilon - \delta_{SW}}{\tau}\right) + \left(\frac{\varepsilon}{Sr} * \frac{\Delta Sr}{\Delta t}\right)$$

where δ_{SW} and δ_{IN} are the $\delta^{88/86}$Sr of seawater and of Sr input to the ocean, respectively, ε is the isotopic offset during Sr incorporation into $CaCO_3$, τ is the e-folding time scale for δ_{SW} to relax toward isotopic steady state (i.e., if Sr inventory is at steady state, then τ equates to the residence time of Sr in the ocean), and $\Delta\delta_{SW}/\Delta t$ and $\Delta Sr/\Delta t$ are the time derivatives of δ_{SW} and the ocean's Sr inventory, respectively. This expression separates $\delta^{88/86}$Sr changes caused by isotope mass balance when the Sr budget is in balance (the first term) from the $\delta^{88/86}$Sr change caused by an imbalance in the ocean's Sr budget (the second term). Any change in seawater $\delta^{88/86}$Sr may be the result of either of two end-member explanations, changes in δ_{IN} or [Sr], which we consider separately below.

The first end-member explanation posits a balanced Sr budget (i.e., $\Delta Sr/\Delta t = 0$), such that seawater $\delta^{88/86}$Sr change is entirely caused by the first term in Eq. 1, which describes how δ_{SW} relaxes toward a value at which $\delta^{88/86}$Sr of $CaCO_3$ burial (i.e., $\delta_{SW} + \varepsilon$) is equal to δ_{IN}. Therefore, if δ_{IN}, Sr input flux (F_{IN}), and [Sr]

Fig. 2. Sr isotope records over the past 35 Myr. (**A**) Radiogenic Sr isotope record in marine barite separated from several sites over the past 35 Myr (errors are smaller than the symbol size), along with the seawater Sr isotope curve (gray line) from McArthur et al. (13). Slight differences between the curves are likely due to differences in the age models used. (**B**) Stable Sr isotope record of these down-core marine barite samples with a polynomial curve fit (black line) ± 0.02‰ analytical uncertainty (gray lines). All data are provided in table S1. The inferred seawater $\delta^{88/86}$Sr was determined by adding the constant isotopic offset (fractionation) of 0.536‰ based on core-top data. Site 572 is shown in yellow; Site 573, red; Site 574, orange; Site 575, green; Site 849, purple; Site 1218, dark green; and Site 1219, gray. The average $\delta^{88/86}$Sr core top value (–0.146‰) is marked with a blue star, and the average PC72 value (–0.178‰) is marked with a pink triangle (individual measurements are shown as open pink diamonds because they were not used in the fit); the core-top average is not included in the polynomial fit (see discussion section in the supplementary materials).
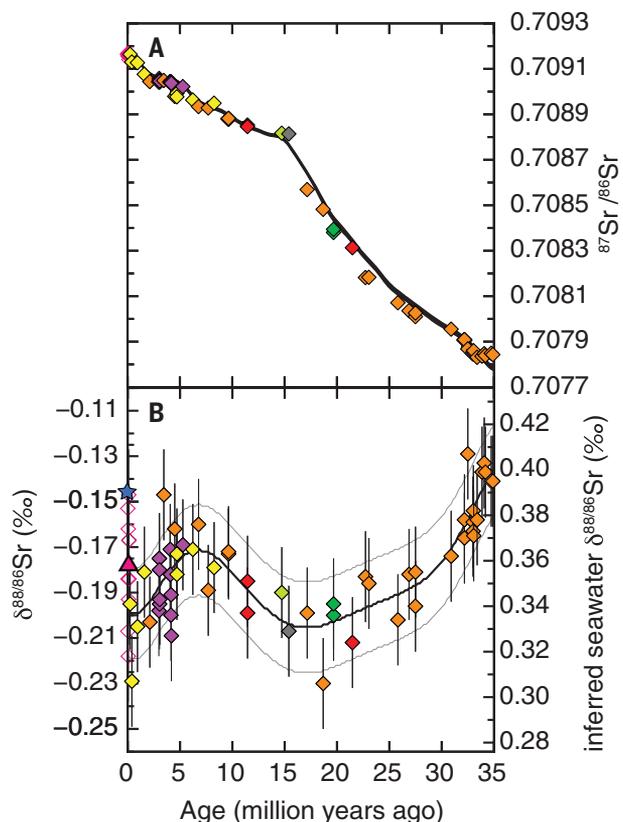
Fig. 3. Sr isotope mass balance model results under the simplifying assumption of constant Sr input to the ocean. The symbols for $\delta^{88/86}Sr$ include all down-core data and the average PC72 value (−0.178‰, as the pink triangle in Fig. 2). The reconstructed seawater Sr/Ca data from Lear et al. (16) are included as + symbols in the bottom panel for comparison. These inverse model results are obtained when Eq. 1 is recast to yield Sr flux imbalance as a function of reconstructed δ_{SW} and then integrated backward in time. This approach demonstrates that the δ_{SW} data are a strong constraint on the fluctuations in the Sr mass balance, but that the integrated long-term trend in the Sr inventory depends mainly on the values chosen for δ_{IN} and for ε. Uncertainties in δ_{IN} and ε were propagated using a Monte Carlo approach, with individual runs shown in red or blue when $\delta_{IN} - \varepsilon$ was either greater or less than

the long-term mean of our δ_{SW} record, respectively. See fig. S2 for more details and for the results of a forward model in which δ_{SW} is calculated from Eq. 1 using the time-varying Sr imbalance adjusted to a mean of zero to remove the long-term trend in the Sr inventory. The key outcome of this model-based analysis is that our seawater $\delta^{88/86}Sr$ record is a strong constraint on changes in seawater Sr mass balance even if the secular Sr inventory trend cannot be reconstructed on the basis of our data alone.
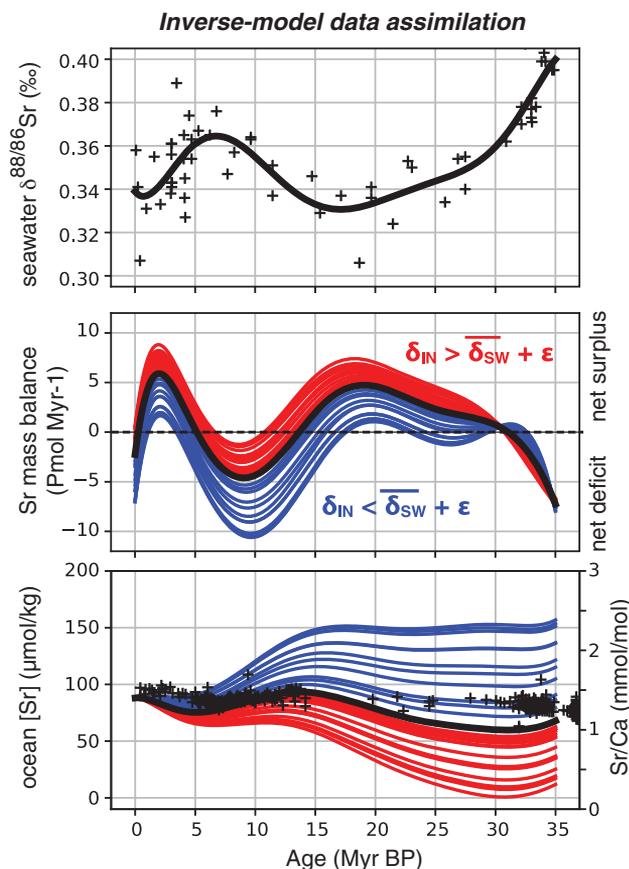
were taken to be constant, then δ_{SW} would adjust over a few million years (i.e., 2 to 3 e-folding τ) and then remain constant at a value of $\delta_{IN} - \varepsilon$. This is in stark contrast to the observed variations in the $\delta^{88/86}Sr$ record. If, however, δ_{IN} is continuously changing, then the $\delta^{88/86}Sr$ record could be explained by the resulting continuous adjustments of δ_{SW}. This scenario would result in a strong, positively coupled signal in $^{87}Sr/^{86}Sr$, which we do not see. Such hypothetical changes in δ_{IN} are plausible given the spread in $\delta^{88/86}Sr$ from weathering of silicate rocks or limestone [typical $\delta^{88/86}Sr$ of 0.58 and 0.18‰, respectively (7)], the relative contribution of which may have changed over time. This hypothetical end-member scenario posits neither constant weathering Sr flux nor constant Sr burial but instead requires that Sr input and output be equal, yielding a balanced Sr budget.

The second end-member explanation posits that seawater $\delta^{88/86}Sr$ changes reflect transient imbalances in the ocean's Sr budget represented by the second term in Eq. 1. If Sr input exceeds outputs (i.e., $\Delta Sr/\Delta t > 0$), then δ_{SW} will transiently decline toward δ_{IN}, whereas if Sr

output exceeds input (i.e., $\Delta Sr/\Delta t < 0$), then δ_{SW} will transiently increase because of the isotopic fractionation during Sr incorporation into $CaCO_3$ and the associated isotopic Rayleigh distillation of the residual ocean Sr inventory. Because the magnitude of fractionation is large, even modest Sr budget imbalances will impart substantial transient changes in δ_{SW}. Given that Sr input and output are expected to change independently with changing climate and sea level, we regard this explanation (transient changes caused by budget imbalance) as the likely dominant driver of the seawater $\delta^{88/86}Sr$ changes.

Seawater Sr and carbonate deposition

To illustrate the power of seawater $\delta^{88/86}Sr$ in constraining carbonate deposition, we make the simplifying assumption that the bulk Sr input flux and its stable isotopic composition are constant through time to solve for Sr output and numerically integrate the Sr budget back through time (Fig. 3). We applied a Monte Carlo approach to assess the impact of uncertainty in the value of both δ_{IN} (2σ of 0.02‰) and ε (2σ of 0.01‰) (see the supplementary materials for details). Our analysis yields Sr budget imbal-

ances that coherently oscillate by ±5 Pmol Myr^{-1} (10^{15} mol Myr^{-1}) to create the oscillations in our $\delta^{88/86}Sr$ data, but the integrated secular [Sr] cannot be determined within simulated uncertainty (Fig. 3). Taking existing seawater Sr/Ca reconstructions (16) as evidence that there was no secular [Sr] trend over the past ~35 Myr, the oscillating Sr budget imbalance still integrates to up to ±25% Sr inventory oscillations (±25 Pmol; fig. S2B), with a maximum during the Middle Miocene and minima during the Oligocene and Pliocene. If these Sr budget changes were all due to changes in net $CaCO_3$ deposition, then our model results would imply fluctuations in the order of ±13% in the rate of net $CaCO_3$ burial [calculated relative to a rate of 38 Pmol Myr^{-1} (6)]; however, this value can vary considerably depending on the ratio of aragonite to calcite deposition. For example, if we attribute all of the change to deposition or weathering and/or diagenesis of aragonitic shelf carbonates with 8000 ppm Sr (17), then our modeled imbalance fluxes of ±5 Pmol Myr^{-1} would correspond to ±7.5 TgC yr^{-1} changes in net burial [i.e., only about ±5% of the mean Holocene estimated shelf burial flux, assuming 150 TgC yr^{-1} total shelf burial; see (18) and references therein].

Considering that changes in $^{87}Sr/^{86}Sr$ and $\delta^{88/86}Sr$ do not vary uniformly over time (Fig. 4) (i.e., the records do not correlate), this is consistent with the high sensitivity of $\delta^{88/86}Sr$ compared with $^{87}Sr/^{86}Sr$ to neritic carbonate deposition and/or recrystallization. As diagnosed by our model, changes in the $\delta^{88/86}Sr$ of seawater respond mainly to changes in the ocean's Sr inventory, such as through changing carbonate burial, whereas the $^{87}Sr/^{86}Sr$ system is insensitive to Sr inventory changes. Conversely, increased weathering of granitic (or basaltic) rocks on land will have a large effect on $^{87}Sr/^{86}Sr$, with relatively little impact on $\delta^{88/86}Sr$ as long as the weathering change does not drive a large Sr budget imbalance. Thus, the paired records of $\delta^{88/86}Sr$ and $^{87}Sr/^{86}Sr$ provide an invaluable constraint in assessing changes in both continental weathering and the rate and extent of global carbonate burial (6).

Our record demonstrates that between 35 and ~25 Ma, when $\delta^{88/86}Sr$ of seawater decreased from −0.406 to −0.336‰ but the change in $^{87}Sr/^{86}Sr$ was small, the dominant process affecting seawater [Sr] and isotope ratios was a decrease in neritic carbonate deposition possibly because of a drop in sea level over the Oligocene (19). Over the following 10 million years (~25 to 15 Ma), $^{87}Sr/^{86}Sr$ increased (from 0.7082 to 0.7088), whereas $\delta^{88/86}Sr$ changes were small, suggesting an increase in the input of Sr from rocks with more radiogenic $^{87}Sr/^{86}Sr$ relative to input from basaltic weathering or seafloor hydrothermal sources. This is consistent with some estimates for increased erosion in the Western Greater Himalaya, as well as the
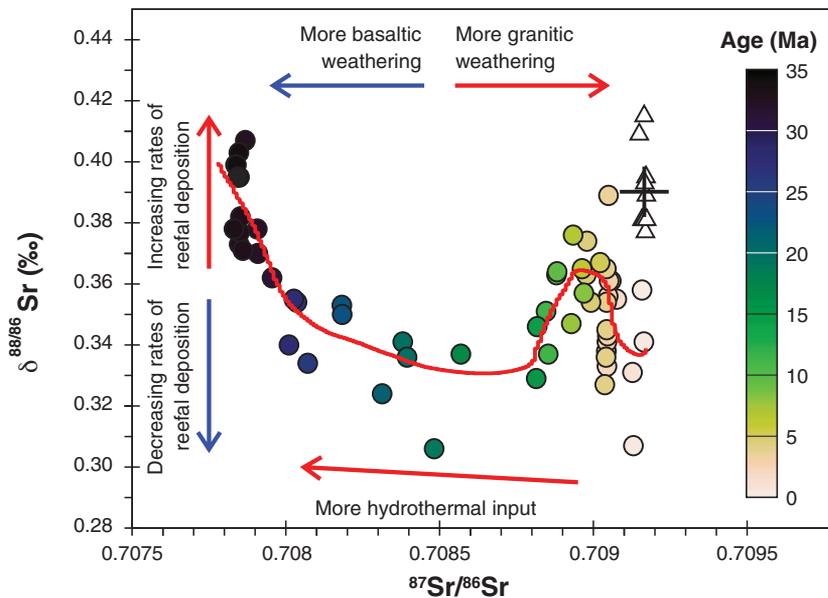
Fig. 4. Observed evolution of the Sr system in radiogenic versus stable Sr isotope space over the past 35 Myr. Circles reflect down-core barite measurements and are color-coded by sample age, and triangles reflect the core-top measurements. The cross indicates modern seawater Sr isotopic composition. All barite data are corrected for the isotopic fractionation offset of 0.536‰, and the x- and y-axis scales reflect inferred seawater Sr isotopic composition rather than measured $^{87}Sr/^{86}Sr$ and $\delta^{88/86}Sr$ of barite. The red line represents the polynomial fit to the data presented in Fig. 2. The colored arrows illustrate the approximate direction in $^{87}Sr/^{86}Sr$ and $\delta^{88/86}Sr$ space of the seawater Sr response to some of the key controlling factors: the proportion of basaltic versus granitic weathering, the hydrothermal Sr input flux to the ocean, and rates of reef $CaCO_3$ deposition.

initiation (or intensification) of the Asian monsoon in the Early Miocene (*20, 21*). In the Middle to Late Miocene (~15 to 5 Ma), $\delta^{88/86}Sr$ increased, indicating an increase in carbonate deposition coincident with the proliferation of coral reefs (*22*) and an increase in pelagic carbonate sedimentation in the Middle Miocene (*23*). This was likely accompanied by a decrease in the rate of erosion in the Himalaya and Alps (*24, 25*) (because $^{87}Sr/^{86}Sr$ increases at a slower rate). Finally, the last 5 Myr of the record saw a decrease in $\delta^{88/86}Sr$ to the Pleistocene average of about –0.186‰, suggesting a decrease in neritic carbonate burial (or increase in shelf carbonate diagenesis) associated with a drop in sea level and the development of Northern Hemisphere glaciation (potentially with large short-term fluctuations, as indicated by the large range of $\delta^{88/86}Sr$ in the Pleistocene and the present-day Sr imbalance). One implication of this coupled record is that we do not see a continuous increase in carbonate deposition (which would be manifested in a continuous increase in $\delta^{88/86}Sr$), as would be expected from a monotonous increase in chemical weathering and increased delivery of weathering products (alkalinity) to the ocean over the past 35 Myr.

Although changes in seawater $\delta^{88/86}Sr$ provide important insights into the Sr cycle and suggest that $CaCO_3$ burial and [Sr] have fluctuated considerably over the past 35 Myr, the

system is underconstrained. Interpretations of the Sr isotope records can be refined if seawater [Sr] or the carbonate deposition history were known. Previous attempts to reconstruct seawater [Sr] (*16, 26–32*), however, yielded conflicting records. Moreover, most of these records reported Sr/Ca ratios, and converting Sr/Ca in mineral deposits to seawater [Sr] involves many assumptions (e.g., unchanging or known seawater Ca concentrations) and corrections (e.g., vital effects and post deposition alteration). The record with highest resolution over the past 35 Myr (*16*) shows fluctuations in Sr/Ca that generally correspond in timing with changes in the $\delta^{88/86}Sr$, although with smaller magnitude (Fig. 3). Specifically, Lear *et al.* (*16*) showed that seawater Sr/Ca rose gradually through the Oligocene and Early Miocene, followed by a decrease until the Late Miocene and a subsequent increase toward the present day. If this Sr/Ca record is representative of seawater [Sr], then it is consistent with measurable fluctuations in seawater $\delta^{88/86}Sr$, as described above. On the basis of our model, the total Sr inventory in the ocean could have changed by up to 25%, fluctuating between ~66 and 110 μM around the present-day concentration of ~88 μM (fig. S2B). Although these changes are much larger than those calculated by Lear *et al.* (*16*), which were based on benthic foraminifera Sr/Ca ratios, some of

this discrepancy may be related to the many assumptions involved in both our model and those associated with the conversion of foraminifera Sr/Ca ratios to [Sr]. We note that a change in [Sr] in the range of 25 μM over 10 to 20 million years is easily attainable considering the vast amount of Sr stored in neritic carbonates and changes in sea level that subject these deposits to deposition or recrystallization processes. These changes in [Sr] have some implications to the $^{87}Sr/^{86}Sr$ as well. The sensitivity to any changes in the input flux of Sr depends on the [Sr] in the ocean; the larger the reservoir, the more difficult it is to change, so any response to perturbation will be smaller (lower sensitivity). Therefore, [Sr] will modulate the slope of change in $^{87}Sr/^{86}Sr$. For example, between 35 and 25 Ma, when the seawater $\delta^{88/86}Sr$ decreased and thus [Sr] increased, it gradually becomes more difficult to change the Sr isotope ratios in seawater (both $^{87}Sr/^{86}Sr$ and $\delta^{88/86}Sr$). The reasonable agreement between our inferred Sr inventory changes and completely independent estimates from the Sr/Ca dataset by Lear *et al.* (*16*) is strong evidence that these (independent) records are consistent. That means that we now have internally consistent and orthogonal constraints on $\delta^{88/86}Sr$ and [Sr] through much of the Cenozoic, reducing by one the degrees of freedom of the system for the purpose of data assimilation.

Conclusions and implications

Because seawater $\delta^{88/86}Sr$ is sensitive to shallow water carbonate deposition and/or recrystallization (*33*), it provides a globally integrated estimate for the extent of reef and associated changes in carbonate depositional rates (e.g., *34-35*) (see the supplementary materials). Thus, if the global rate of carbonate burial in deep-sea sediments is also known, for example, by interpreting changes in the calcite compensation depth (CCD) [(*36–38*) but see (*39*) for a discussion of how CCD and global deep-sea burial rates can be decoupled], then combining records of changes in the CCD with $\delta^{88/86}Sr$ could give a measure of the total global carbonate burial rate. At steady state, this must equal total global terrestrial carbonate plus silicate weathering and net seafloor input of Ca^{2+} and/or Mg^{2+}; (hereafter, "alkalinity"), thus resolving the entire inorganic carbon budget of surficial Earth. The $\delta^{88/86}Sr$ record could be explained by fluctuations in the total amount and location of carbonate deposition, and the associated alkalinity changes (if any) may be derived from carbonate weathering or deposition of shelf carbonates (*23, 35*), thus not necessarily requiring large changes in silicate weathering (*40, 41*). Overall, $\delta^{88/86}Sr$ data provide constraints and insights into the inner workings of the global carbon cycle, and in conjunction with radiogenic Sr and other proxies raise the prospect of quantifying changes

in global carbonate burial through time. This in turn enables, with more detailed modeling of the coupled stable and radiogenic Sr, constraining the silicate weathering feedback that links atmospheric p_{CO_2} and temperature and thus unraveling the explanation for the generally declining trends in global temperature and atmospheric p_{CO_2} that have occurred over the Late Cenozoic.

REFERENCES AND NOTES

1. H. Elderfield, *Treatise on Geochemistry, Volume 6: The Oceans and Marine Geochemistry* (Elsevier, 2006).
2. R. A. Berner, *Am. J. Sci.* **294**, 56–91 (1994).
3. G. E. Ravizza, J. C. Zachos, "Records of Cenozoic ocean chemistry," in *Treatise on Geochemistry, Volume 6: The Oceans and Marine Geochemistry* (Elsevier, 2006), pp. 551–582.
4. G. Li, H. Elderfield, *Geochim. Cosmochim. Acta* **103**, 11–25 (2013).
5. A. Krabbenhöft *et al.*, *Geochim. Cosmochim. Acta* **74**, 4097–4109 (2010).
6. H. Vollstaedt *et al.*, *Geochim. Cosmochim. Acta* **128**, 249–265 (2014).
7. C. R. Pearce *et al.*, *Geochim. Cosmochim. Acta* **157**, 125–146 (2015).
8. J. Fietzke, A. Eisenhauer, *Geochem. Geophys. Geosyst.* **7**, Q08009 (2006).
9. I. H. Widanagamage, E. A. Schauble, H. D. Scher, E. M. Griffith, *Geochim. Cosmochim. Acta* **147**, 58–75 (2014).
10. I. H. Widanagamage *et al.*, *Chem. Geol.* **411**, 215–227 (2015).
11. E. M. Griffith, A. Paytan, U. G. Wortmann, A. Eisenhauer, H. D. Scher, *Chem. Geol.* **500**, 148–158 (2018).
12. W. Broecker, K. Matsumoto, E. Clark, I. Hajdas, G. Bonani, *Paleoceanography* **14**, 431–436 (1999).
13. J. M. McArthur, R. J. Howarth, G. A. Shields, "Strontium isotope stratigraphy," in *The Geologic Time Scale*, F. M. Gradstein, J. G. Ogg, M. Schmitz, G. Ogg, G. Eds. (Elsevier 2012), pp. 127–144.
14. A. C. Davis, M. J. Bickle, D. A. H. Teagle, *Earth Planet. Sci. Lett.* **211**, 173–187 (2003).
15. D. Vance, D. A. H. Teagle, G. L. Foster, *Nature* **458**, 493–496 (2009).
16. C. H. Lear, H. Elderfield, P. A. Wilson, *Earth Planet. Sci. Lett.* **208**, 69–84 (2003).
17. D. J. J. Kinsman, H. D. Holland, *Geochim. Cosmochim. Acta* **33**, 1–17 (1996).
18. O. Cartapanis, E. D. Galbraith, D. Bianchi, S. L. Jaccard, *Clim. Past* **14**, 1819–1850 (2018).
19. M. A. Kominz, W. A. Van Sickel, K. G. Miller, J. V. Browning, "Sea-level estimates for the latest 100 million years: One-dimensional backstripping of onshore New Jersey borehole," in *Sequence Stratigraphic Models for Exploration and Production: Evolving Methodology, Emerging Models and Application Case Histories*, J. M. Armentrout, N. C. Rosen, Eds. (SEPM Society for Sedimentary Geology, 2002), vol. 22, pp. 303–315.
20. P. D. Clift *et al.*, *Nat. Geosci.* **1**, 875–880 (2008).
21. A. A. Webb *et al.*, *Lithosphere* **9**, 637–651 (2017).
22. W. Kiessling, *Annu. Rev. Ecol. Evol. Syst.* **40**, 173–192 (2009).
23. B. N. Opdyke, B. H. Wilkinson, *Paleoceanography* **3**, 685–703 (1988).
24. N. S. Vögeli, P. van der Beek, M. Huyghe, Y. Najman, *J. Geol.* **125**, 515–529 (2017).
25. S. D. Willett, *Annu. Rev. Earth Planet. Sci.* **38**, 411–437 (2010).
26. D. W. Graham, M. L. Bender, D. F. Williams, L. D. Keigwin Jr., *Geochim. Cosmochim. Acta* **46**, 1281–1292 (1982).
27. T. Steuber, J. Veizer, *Geology* **30**, 1123–1126 (2002).
28. L. C. Ivany *et al.*, *J. Sediment. Res.* **74**, 7–19 (2004).
29. A. K. Tripati, W. D. Allmon, D. E. Sampson, *Earth Planet. Sci. Lett.* **282**, 122–130 (2009).
30. R. M. Coggon, D. A. H. Teagle, C. E. Smith-Duque, J. C. Alt, M. J. Cooper, *Science* **327**, 1114–1117 (2010).
31. V. Balter, C. Lécuyer, J.-A. Barrat, *Palaeogeogr. Palaeoclimatol. Palaeoecol.* **310**, 133–138 (2011).
32. S. M. Sosdian *et al.*, *Geochem. Geophys. Geosyst.* **13**, Q10014 (2012).
33. H. M. Stoll, D. P. Schrag, *Geochim. Cosmochim. Acta* **62**, 1107–1118 (1998).
34. A. B. Ronov, *Stratisphere or Sedimentary Envelope of the Earth: A Quantitative Study* [in Russian] (Nauka, 1993).
35. B. N. Opdyke, J. C. G. Walker, *Geology* **20**, 733–736 (1992).
36. T. H. Van Andel, *Earth Planet. Sci. Lett.* **26**, 187–194 (1975).
37. H. Pälike *et al.*, *Nature* **488**, 609–614 (2012).
38. S. M. Campbell, R. Moucha, L. A. Derry, M. E. Raymo, *Geochem. Geophys. Geosyst.* **19**, 1025–1034 (2018).
39. S. E. Greene *et al.*, *Paleoceanogr. Paleoclimatol.* **34**, 930–945 (2019).
40. J. K. Willenbring, F. von Blanckenburg, *Nature* **465**, 211–214 (2010).
41. J. K. Caves, A. B. Jost, K. V. Lau, K. Maher, *Earth Planet. Sci. Lett.* **450**, 152–163 (2016).

SUPPLEMENTARY MATERIALS

science.sciencemag.org/content/371/6536/1346/suppl/DC1
Materials and Methods
Supplementary Text
Figs. S1 and S2
Table S1
References (*42–55*)

Science

A 35-million-year record of seawater stable Sr isotopes reveals a fluctuating global carbon cycle

Adina Paytan, Elizabeth M. Griffith, Anton Eisenhauer, Mathis P. Hain, Klaus Wallmann and Andrew Ridgwell

Carbon cycle history

Marine carbon includes organic and inorganic components, both of which must be accounted for to understand the global carbon cycle. Paytan *et al.* assembled a record of stable strontium isotopes (^{88}Sr and ^{86}Sr) derived from pelagic marine barite and used it to reconstruct changes in the deposition and burial of biogenic calcium carbonate in marine sediments. These data, when combined with measurements of $^{87}Sr/^{86}Sr$, can help to reveal past changes in the sources and sinks of strontium, as well as variations in carbonate deposition that affect the carbon cycle.

Science, this issue p. 1346

ARTICLE TOOLS	http://science.sciencemag.org/content/371/6536/1346
SUPPLEMENTARY MATERIALS	http://science.sciencemag.org/content/suppl/2021/03/24/371.6536.1346.DC1
REFERENCES	This article cites 47 articles, 11 of which you can access for free http://science.sciencemag.org/content/371/6536/1346#BIBL
PERMISSIONS	http://www.sciencemag.org/help/reprints-and-permissions